Available online at www.sciencedirect.com
SCIENCE DIRECT®
Estuarine, Coastal and Shelf Science 69 (2006) 291–298
ESTUARINE COASTAL AND SHELF SCIENCE
www.elsevier.com/locate/ecss

The sediment trapping efficiency of the macro-tidal Daly Estuary, tropical Australia

E. Wolanski [a,*], D. Williams [b], E. Hanert [c]

[a] Australian Institute of Marine Science, PMB No. 3, Townsville MC, Queensland 4810, Australia
[b] Department of Natural Resources, Environment and The Arts, PO Box 30, Palmerston 0831, Northern Territory, Australia
[c] Department of Meteorology, The University of Reading, Earley Gate, Reading RG6 6BB, UK

Received 4 August 2005; accepted 19 April 2006
Available online 27 June 2006

Abstract

Field studies were carried out on the water and sediment dynamics in the tropical, macro-tidal, Daly Estuary. The estuary is shallow, very-turbid, about 100 km long, and the entrance is funnel-shape. In the wet, high flow season, normal tidal ranges can be suppressed in the estuary, depending on inflow rates, and freshwater becomes dominant up to the mouth. At that time a fraction of the fine sediment load is exported off-shore as a bottom-tagging nepheloid layer after the sediment falls out of suspension of the thin, near-surface, river plume. The remaining fraction and the riverine coarse sediment form a large sediment bar 10 km long, up to 6 m in height and extending across the whole width of the channel near the mouth. This bar, as well as shoals in the estuary, partially pond the mid- to upper-estuary. This bar builds up from the deposition of riverine sediment during a wet season with high runoff and can raise mean water level by up to 2 m in the upper estuary in the low flow season. This ponding effect takes about three successive dry years to disappear by the sediment forming the bar being redistributed all over the estuary by tidal pumping of fine and coarse sediment in the dry season, which is the low flow season. The swift reversal of the tidal currents from ebb to flood results in macro-turbulence that lasts about 20 min. Bed load transport is preferentially landward and occurs only for water currents greater than 0.6 m s^{-1}. This high value of the threshold velocity suggests that the sand may be cemented by the mud. The Daly Estuary thus is a leaky sediment trap with an efficiency varying both seasonally and inter-annually.
© 2006 Elsevier Ltd. All rights reserved.

Keywords: sediment budget; flocculation; suspended sediment; bed load; tidal symmetry; ponding

1. Introduction

Since the pioneer work on estuarine dynamics by Pritchard (1952, 1967) and Postma (1967), processes such as tidal asymmetries (duration and peak velocity), baroclinic currents, storms, and human activities such as dredging, channelisation and hard structures, have been understood to result in patterns of deposition and erosion that make estuaries change and evolve on a wide range of time scales (Dyer, 1986, 2000; Perillo, 2000; FitzGerald and Knight, 2005). This knowledge led to the realization that estuaries are sediment traps. This trap is not 100% efficient, i.e. estuaries infill but still export some fine and coarse sediment particularly during periods of high river flow (Syvitski et al., 2005). The trapping and export have been well documented for fine, cohesive sediment in micro- and meso-tidal estuaries (Dyer, 2000; FitzGerald and Knight, 2005). The export of riverine fine sediment is poorly understood in macro-tidal estuaries since these estuaries import coastal fine sediment by tidal pumping (Chappell, 1993; Chappell and Woodroffe, 1994; Woodroffe, 2003; Wolanski, 2006). The estuarine trapping and export of riverine sand are barely understood (Milliman and Meade, 1983). In some estuaries the riverine coarse sediment (sand) may not reach the coast (Bryce et al., 1998), while in others the sand is exported to coastal waters and the continental shelf (FitzGerald et al., 2005). One reason for the difficulty in assessing sand transport

* Corresponding author.
E-mail address: e.wolanski@aims.gov.au (E. Wolanski).

0272-7714/$ - see front matter © 2006 Elsevier Ltd. All rights reserved.
doi:10.1016/j.ecss.2006.04.023

is that there are no instruments to non-intrusively measure the bed load transport. Instead the net bed load has to be determined indirectly by methods such as grain size analysis, magnetism, and repeated bathymetric surveys to assess changes in sediment storage, and the direction of sand transport has to be inferred from the shape of sand shoals and asymmetries in bed forms (FitzGerald and Knight, 2005).

This paper reports on the case study of the macro-tidal Daly Estuary in tropical Australia (Fig. 1). The estuary is about 100 km long and the spring tidal range is about 6 m at the mouth. A strong tidal asymmetry exists in upper estuary in the dry season, with a small (0.3 m) tidal bore occurring at spring tides (Wolanski et al., 2004). The large catchment area (52,577 km^2) results in occasional major river floods, the largest peaking at about 8,200 m^3 s^{-1} in January 1998. The river is perennial due to spring discharge from limestone aquifers. The wet season occurs between January and April, the dry season during May to September, the remaining months are transitional periods. There are large seasonal and interannual fluctuations of the runoff. It is shown that the estuary exports riverine fine sediment during the high flow season while much of the sand and the remaining fine sediment fraction deposits near the mouth. The deposit can be up to 3 m high, 10 km long and extending across the full width of the estuary. This forms shoals offshore and in the lower estuary that partially pond the mid- and upper-estuary during the dry season. The sediment from these shoals is advected landward back into the estuary by tidal pumping during the dry season. The tidal pumping of the coarse sediment appears to be hindered by cementing by the clay. It takes about 3 dry years—i.e. 3 years of small river sediment inflow following 1 year of high sediment inflow—for this sediment shoal at the mouth to be removed and the sediment redistributed all over the estuary and the tidal ponding effect to disappear.

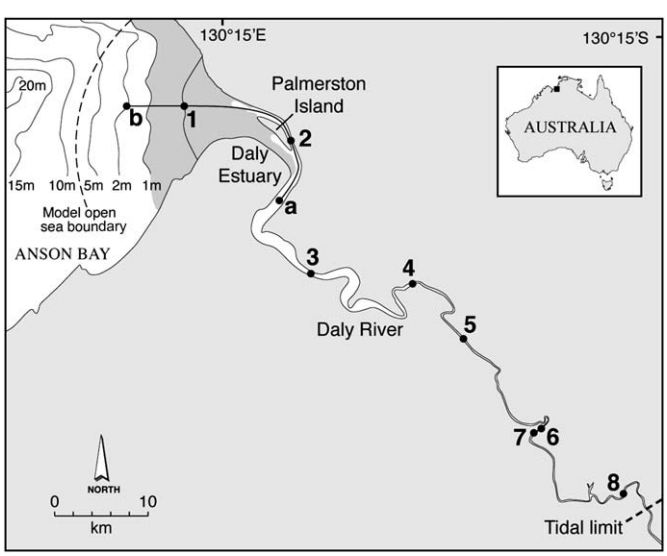

Fig. 1. A location map of the Daly Estuary and key measurement sites.

2. Methods

Monthly-averaged river discharges at Mt. Nancar, upstream of the tide limit, were available for the period 1970–2005. Half-hourly tidal elevation data at site 5 were available for the period 1968–1986.

Field studies were carried out during the dry season in August 2004, November 2004, and September 2005, and in the wet season in March 2005.

In all cruises vertical profiles of salinity, temperature and suspended sediment concentration (SSC) were collected at a number of sites in along-axis transects using a SeaBird CTD equipped with an Analite nephelometer.

In March 2004 moorings were deployed for 3 days at sites b and 1 (see a location map in Fig. 1), equipped with Nortek and RDI ADCP current meters cum tide gauges, SBE 16 salinometer-temperature recorders, and nephelometers spread from top to bottom.

In August 2004, Seabird and Diver tide gauges were bottom-mounted for 1 month at sites 2, 5, 6 and 8.

In November 2004, a mooring was maintained for 3 days at site 1, equipped with a S4 current meter, and SBE 16 and three nephelometers.

In September 2005, moorings were maintained for 1 week at sites 2–7 containing Nortek and ADCP RDI, SBE 26 tide gauges, SBE 16, and nephelometers.

The nephelometers were equipped with wipers cleaning the sensor every 30 min. No biological fouling was observed, probably because of the high turbidity in the area. The nephelometers were calibrated in-situ. The instruments saturated at about 30 kg m^{-3}.

The instruments logged data at 5 min intervals.

On one occasion a downward looking ADCP with bottom-tracking mode enabled was deployed on a frame at site 3, 1.5 m off the bottom, to measure the bed load velocity, logging every second. Another ADCP pointing upwards at site 5 logged velocity data every second.

Samples for microscopic observations of suspended particles were obtained using the technique of Ayukai and Wolanski (1997). The samples were examined under an Olympus inverted microscope with a Sony CCD video camera. The images were captured digitally.

A vertically and laterally-averaged 1-D discontinuous finite element model was used to model the dry season hydrodynamics of the estuary. This model is based on the discontinuous Riemann–Galerkin approach suggested by White et al. (2006). As the discrete surface elevation and velocity may exhibit discontinuities between grid cells, the model is able to accurately represent solutions with sharp gradients and even tidal bores. The upstream boundary was the river discharge at the tidal limit and the downstream boundary condition were the tidal elevations applied at the seaward limit of the model shown in Fig. 1.

3. Results

The monthly-averaged river discharge Q_f fluctuated seasonally and inter-annually (Fig. 2). Peak flow occurred in the wet

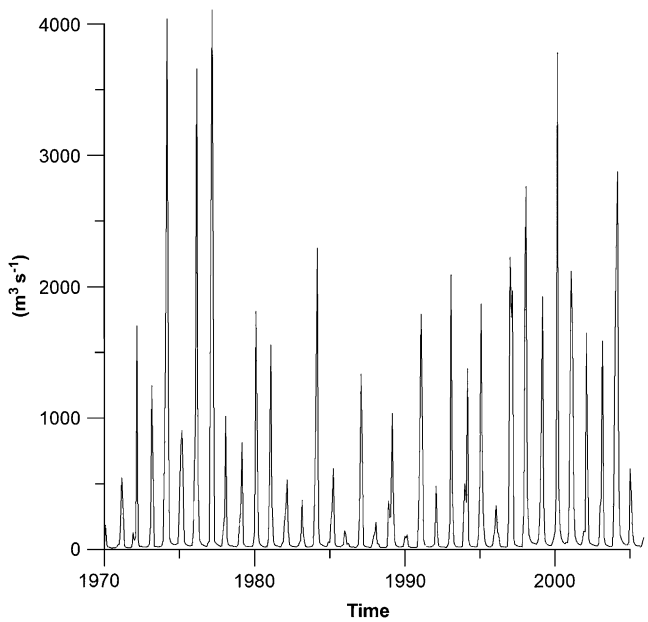

Fig. 2. Time-series plot of the monthly-averaged Daly River discharge.

season, the maximum value was 4038 $m^3 s^{-1}$ in 1974 and the minimum value was 183 $m^3 s^{-1}$ in 1970, i.e. with an inter-annual variation ratio of 22. There are thus wet years and dry years. The smallest flows occurred in the dry season, the maximum value was 35 $m^3 s^{-1}$ in 1974 and the minimum value was 11 $m^3 s^{-1}$ in 1970, i.e. with an inter-annual variation ratio of about 3.

When the river discharge exceeds 3000 $m^3 s^{-1}$, the tides in the mid- to upper-estuary are suppressed (Fig. 3). In the dry season the minimum tidal elevation in the mid-estuary varied inter-annually by about 2 m (Fig. 4).

The tides at site 1 in August–September 2004, in the dry season, were exactly those predicted from the Admiralty charts and showed no tidal asymmetry. Further upstream, the tides became increasingly asymmetric and decreased in amplitude with increasing distance from site 1 (not shown). At site 2, the spring tide was already asymmetric, the ebb tide lasting 1 h longer than the flood tide. At site 5, the spring tides were

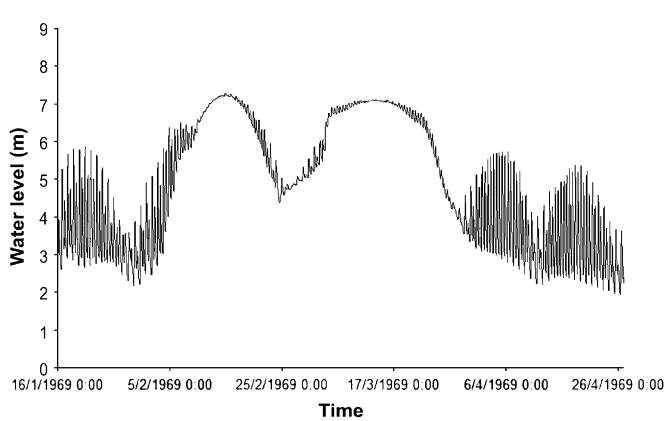

Fig. 3. Time-series plot during the 1969 wet season of the water level at site 5 (see a location map in Fig. 1).

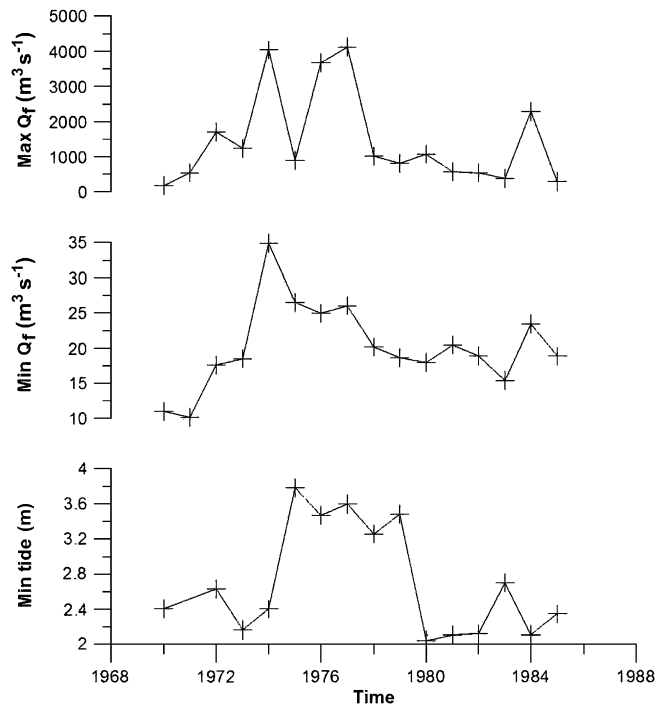

Fig. 4. Time-series of the maximum and minimum monthly-averaged river discharge Q_f and of the minimum tidal elevation at site 5 (see a location map in Fig. 1).

already 1.5 m smaller than those at the mouth and lasted 2 h longer at ebb than at flood tides. At site 6 the spring tides were 2 m smaller than those at the mouth and lasted 3 h longer at ebb than at flood tide. At site 8 the spring tides were only 0.8 m and the flood tide lasted only 1 h. Further during a spring–neap tide cycle the high tide elevation fluctuated much more than the low tide fluctuation; in addition the low tide elevation was also higher during spring tide than during neap tide while the high tide elevation was higher at spring tide than at neap tide (Fig. 5).

The estuary fluctuated seasonally between stratified to well-mixed conditions. During the dry season in November 2004, the waters were vertically homogenous in temperature (not shown) and salinity while it was stratified in suspended sediment concentration (SSC) near the mouth (Fig. 6).

During the wet season in March 2004, the estuary was fresh up to the mouth; it was highly stratified in salinity and SSC offshore from the mouth, with fine sediment settling out of the thin, near-surface, river plume and forming a near-bottom nepheloid layer (Fig. 6). The river plume extended at least 30 km offshore from b (see a location map in Fig. 1) and 20 km northward (not shown), this being the limit of the CTD surveys. The nepheloid layer extended only 10 km offshore (not shown).

In the dry season the tidal currents, salinity and SSC varied along-axis. The peak currents and the tidal asymmetry in currents and SSC increased with increasing distance landward (Fig. 7). At site 1, at the offshore end of the shoal at the mouth, the temperature fluctuated between 31 °C at high tide and 33 °C at low tide, while the corresponding values for salinity

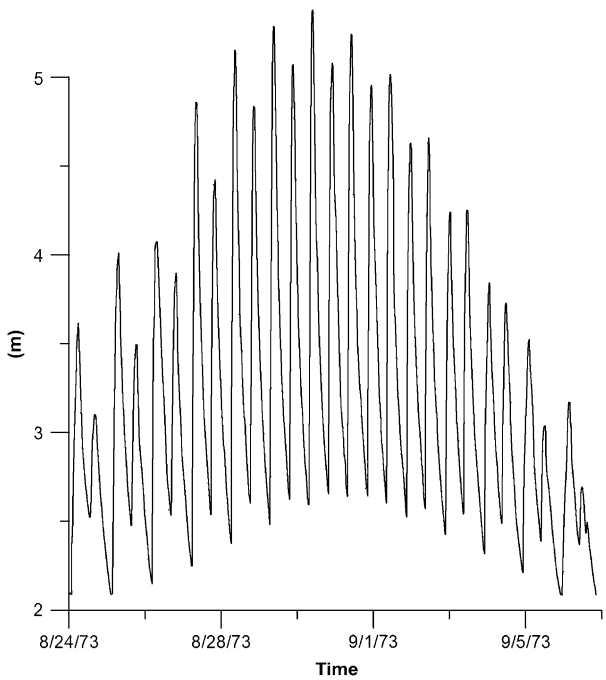

Fig. 5. Time-series plot over a spring-neap tide cycle in the dry season of the water level at site 5. Note that the low tide water level rises during spring tides.

were about 35 and 29 (not shown). The SSC was uni-modal, peaking near slack low tide and at the start of the flood tide at about 8 kg m^{-3} at slack low tide. The net suspended sediment flux was landward. At the mouth at site 2, the salinity varied between 22 at low tide and 29 at high tide. The peak velocity 1 m off the bottom was 0.6 m s^{-1} at ebb tide and 1 m s^{-1} at flood tide. The near-bottom SSC was bimodal, peaking during peak tidal currents, and being nearly twice as large at flood tide than at ebb tide. At site 4 the salinity varied between 0.6 at low tide and 1.8 at high tide. The peak velocity 1 m off the bottom was 1.7 m s^{-1} at flood tide and 0.5 m s^{-1} at ebb tide. The SSC was also bimodal with the tidal currents, and the peak SSC was twice as large at flood than at ebb tide. At all sites in the estuary the maximum SSC occurred just after the start of the flood tide and this lasted about 20 min. This corresponded to a period of about 20 min immediately following the reversal of the tides from ebb to flood (Fig. 8a). This current reversal was very swift, occurring within less than 2 min although a tidal bore was not observed on the occasion. During that period the waters were visually observed to be extremely turbulent with macro-eddies 3–20 m wide. These eddies were initially formed near small obstructions to flow on the shore (Fig. 8a) and spread over the whole width of the estuary. These eddies had a velocity peaking at 0.5 m s^{-1}, i.e. half the velocity of the tidal flow at that time (Fig. 8b). During those events, the SSC was strongly stratified (Fig. 7c). A second stratification period occurred near slack high tide.

The bed load velocity was landward, always small (<0.05 m s^{-1}) and only reliably measurable (>0.005 m s^{-1}) when the water velocity exceeded 0.6 m s^{-1} (Fig. 9).

No sand was observed in suspension in the microscopic observations of suspended particles. The clay particles were not flocculated in freshwater but they flocculated in brackish waters. The floc size did not vary much throughout the brackish water region, the flocs were small (median size $d_{50} < 100$ μm) and the sediment particles were bound together by flocculant organic matter. Clay particles often formed a membrane wrapped around the silt particles. Offshore from Palmerson Island, the fine sediment flocs were attached to colonies (often several hundreds of micrometres in diameter) of phytoplankton, fecal pellets and macroscopic aggregates of apparently biological origin.

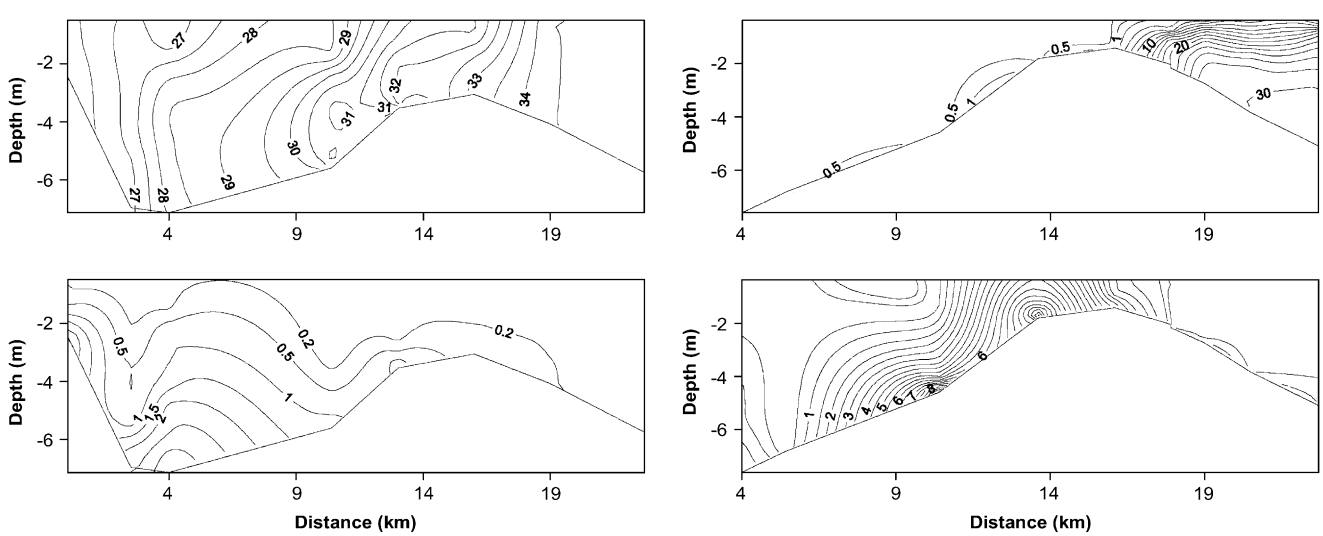

Fig. 6. Along-channel transect at the mouth of (top) salinity and (bottom) suspended sediment concentration (kg m^{-3}) on (left) November 18, 2004 during the dry season at mid-tide, and (right) March 26, 2004 during the wet season at low tide. The survey followed line a–b shown in the location map in Fig. 1. The depths shown are those at the time of the survey.

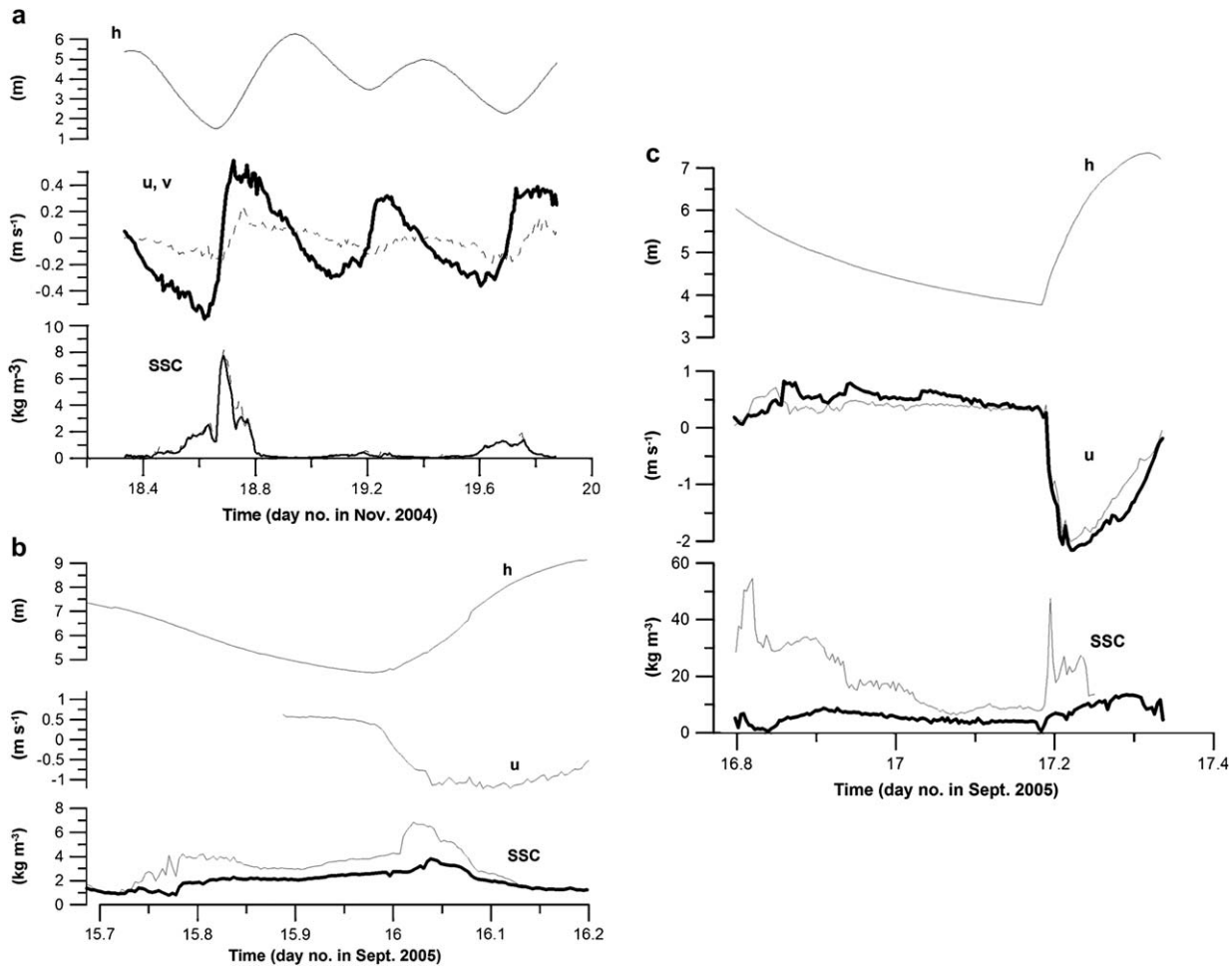

Fig. 7. Time-series plot during the dry season of the depth h, along-axis velocity u (>0 when seaward), and suspended sediment concentration (SSC, kg m^{-3}) at (a) sites 1, (b) site 2, and (c) site 4. See a location map in Fig. 1. In (a) u (line) and v (dashed line) represent eastward and northward velocity. In (a) and (b) the SSC sensors were located about 0.5 and 1 m off the bottom. In (c) the SSC sensors were located 0.5 m off the bottom and 1 m from the surface. The uppermost SSC values are shown as a thick line. Note that at site 1 the tides are symmetric and the SSC is unimodal; the tides become increasingly asymmetric and the SSC become bimodal SSC with increasing distance upstream in the estuary.

4. Discussion

Although the tidal range is 6 m seaward of the offshore shoal, the Daly Estuary is partially ponded in the dry season. This is made apparent by the low tide elevation rising at spring tide. At neap tide the ponded water flows out seaward and the low tide elevation decreases. This is a phenomenon characteristic of shallow, micro- and meso-tidal lagoons (Kjerfve, 1994) and, to our knowledge, has never been reported for macro-tidal estuaries.

The cause of this ponding is the existence of shoals both landward and seaward of the mouth, while the mouth itself is deep (10 m). This ponding is readily apparent from the output of the 1-D model (Fig. 10). The predicted water surface slope is much steeper at flood tide than at ebb tide, and the seawater brought in upstream at the spring flood tide is unable to fully escape at the following ebb tide.

The model also shows the formation of a tidal bore at flood tide in the dry season. This body of water advances up the river with the incoming tide and possesses a well-defined front separating it from the still water in which it advances (Tricker, 1965). The bore is generated just after a shoal, where there is a sudden increase in the flow depth. When the current velocity is large enough, this generates a moving hydraulic jump analogous to a shock wave. Model results are in agreement with these observations of Wolanski et al. (2004) for a freshwater discharge of 20 m^3 s^{-1}. The field data show that the bore does not form for a freshwater discharge of 30 m^3 s^{-1}.

The lack of sediment-laden, transparent exopolymer particles in the turbid Daly Estuary and their presence in the less turbid, coastal waters suggest that the estuary is too turbid for the biology to play a key role in the dynamics of fine sediment while it is important in coastal waters. The Daly Estuary floc dynamics are thus similar to those in other muddy, Australasian estuaries (e.g. Ayukai and Wolanski, 1997; Fabricius and Wolanski, 2000; Wolanski and Spagnol, 2003).

This dry season ponding varies inter-annually by about 2 m. The 1-D model (not shown) suggests that this is due to inter-annual fluctuations of the elevation of the shoals near the mouth by 2.8 m. This ponding occurs in the dry season

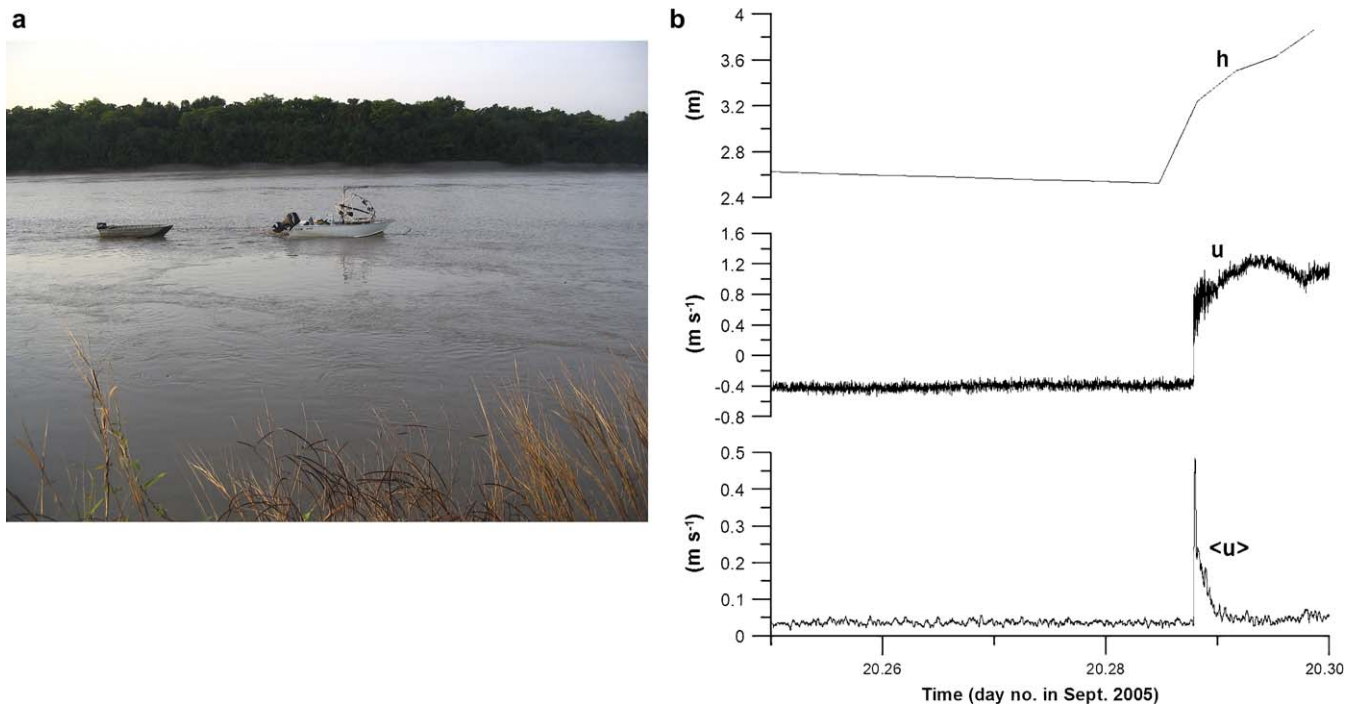

Fig. 8. (a) A photograph of the macro-eddies following the swift current reversal from ebb to flood tide at site 4 on September 17, 2005, during the dry season. (b) Time-series plot during the dry season of the depth h, the 1-min averaged along-axis velocity u (>0 seaward), and the eddy velocity $<u>$ (calculated as the standard deviation of the deviation from the instantaneous current averaged over 1 min) at site 5 during the transition from ebb to flood tide. The eddy velocity is the standard deviation of the residual velocity calculated by subtracting the 10-s averaged velocity from the measured instantaneous velocity.

following a river flood with a mean monthly flow >3000 $m^3 s^{-1}$ (Fig. 4). This demonstrates that the impact of a river flood is not to scour out the estuary by the freshwater, but to build up shoals near the mouth, both offshore and in the lower estuary. The data show that this ponding disappears in about 3 years in the absence of further large floods. This suggests that it takes about 3 years for the currents to redistribute the shoal sediment landward within the estuary.

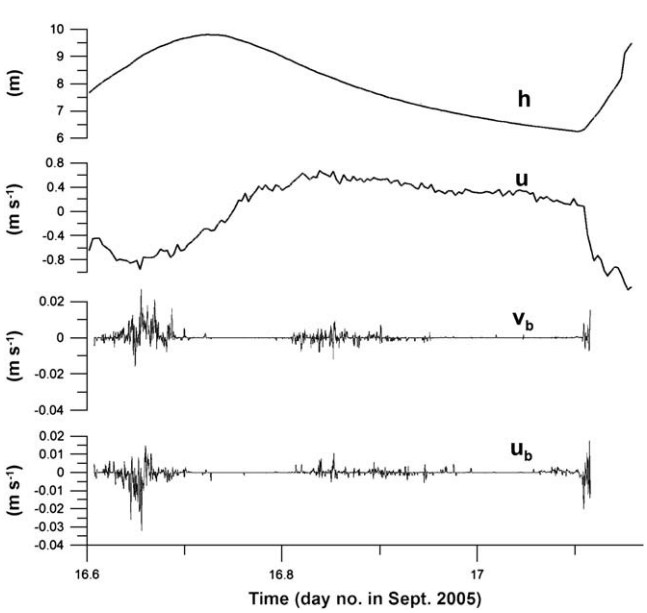

Fig. 9. Time-series plot during the dry season of the depth h, the 1-min averaged mean along-axis velocity u at 1 m off the bottom, and the bed load velocity u_b (eastward) and v_b (northward) at site 3.

In the wet season the Daly Estuary is fresh down to the lower reaches; this observation is in agreement with earlier observations from CTD casts (Chappell and Ward, 1985). The oceanographic mooring data show that during a small to moderate river flood the estuary exports all its riverine fine sediment. However 80% of the riverine fine sediment may settle over the shoal seaward of the mouth. Thus this shoal should be seen as being part of the estuary (Fig. 11a). The remaining 20% may be exported seaward in a near-bottom, nepheloid layer that is formed by the settling of the fine sediment out of the shallow, near-surface, river plume. At this shoal the suspended sediment concentration fluctuates tidally, it peaks at low tide when the turbidity maximum zone that is located in the lower estuary reaches the offshore shoal. A similar tidal advection of the turbidity maximum zone prevails in coastal waters of the Amazon River (Nittrouer and DeMaster, 1986).

In the dry season, the tides decrease in amplitude and increase in asymmetry with distance landward from the mouth, as was documented by Vertessy (1990) and is typical of funnel-shaped, shallow, macro-tidal estuaries (Barry et al., 2006). The tidal velocity asymmetry also increases with distance landward from the mouth. In the mid- and upper-estuary flood tidal currents are twice as large as peak ebb tidal currents. The reversal of the currents from ebb to flood is very swift and is accompanied by a 20-min long period of macro-turbulence with eddies 3–10 m wide and peak velocity of 0.5 m s^{-1}. These eddies were first observed by Wolanski

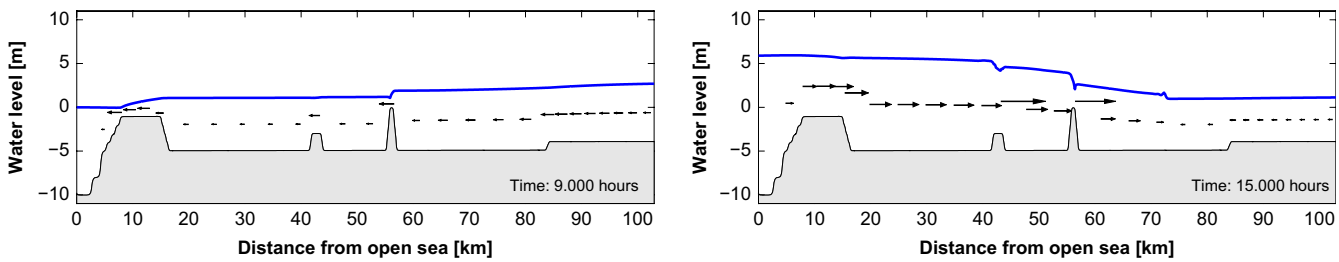

Fig. 10. Snapshots of the 1-D model predictions of ebb (left) and flood (right) tide currents (shown as arrows) and water level elevations (top line) over the complex bathymetry (bottom line) comprising several shoals, for September 2005. The tidal limit is to the right, the sea to the left. At flood tide, a tidal bore is generated. Note the tidal asymmetry of the currents and the virtual cascade over the seaward shoal that is responsible for ponding of the estuary. The locations of the tidal and seaward limits are shown in Fig. 1.

et al. (2004) and remain unexplained. They are important in the transport of fine sediment because, firstly, they erode a large amount of bottom sediment at the start of the rising tide, 1 h before the tidal currents reach their maximum value, and, secondly, they essentially double the suspended sediment concentration. This sediment settles out at ebb tide. No laws are yet available to parameterize this sediment erosion that is not driven by tidal currents. It results in a net landward transport of fine sediment.

Also in the dry season, a weak bed load velocity exists, peaking at about 0.05 m s^{-1} for a near-bottom water velocity of 0.8 m s^{-1}, which is much smaller than that suggested by classical bed load theory (Camenen and Larson, 2005). The threshold velocity for bed load transport is 0.6 m s^{-1}, which is typically 50% higher than that for sand. These findings suggest that the clay may increase the threshold velocity of the sand by cementing the sand–clay matrix, a process that has been observed in laboratory experiments when the pore-filling space is nearly all occupied by mud (Barry et al., 2006). Further the bed load threshold velocity is about 0.6 m s^{-1}, which is much higher than that suggested by classical bed load theory. As a result of the tidal asymmetry, the net bed load transport is landward (Fig. 11b).

Thus in the dry season the fine and coarse net sediment transports are both landward and are presumably responsible for eroding about 2.8 m of the shoals near the mouth within 3 years after their formation following a large river flood.

Thus the Daly Estuary is a leaky sediment trap. The estuarine dynamics and the transport of sediment vary seasonally and interannually. The Daly River sediment load is not measured. The sediment yield from pristine river catchments in tropical Australia is estimated to be 5–15 ton km^{-2} $year^{-1}$ (Chappell and Woodroffe, 1994). If this estimate is valid for Daly River—and this assumption is weak because the catchment is not pristine—the mean Daly riverine sediment inflow into the estuary is $2.5–7.5 \times 10^5$ ton $year^{-1}$. Assuming that there is one large flood every 5 years, the sediment inflow in the estuary from that one flood is $1.25–3.75 \times 10^6$ ton. If all that sediment settles on shoal, the shoal elevation rises by 0.025 m, assuming a density of 2000 kg m^{-3}. The data however suggest that a much higher value, i.e. up to 2.8 m may be deposited in one large flood. Thus either the riverine sediment load is 80 times larger than that predicted by Chappell and Woodroffe, which would point to increased erosion from human land-use or most of the sediment forming the shoal comes from coastal waters during tropical cyclones. Both explanations appear reasonable. Indeed, the increased erosion hypothesis is reasonable from estimates of erosion in other river catchments (Milliman and Meade, 1983; Syvitski et al., 2005). At the rise of the sea level following the end of the ice age, the Daly Estuary flood plains silted at a rate ten times higher than that due to riverine sediment inflow (Chappell, 1993), implying that the bulk of the sediment originated from coastal waters. It should be noted that the estuary meanders actively; the eroding side of the meanders remobilize on the average 2.4×10^5 ton $year^{-1}$ (Wolanski et al., 2004), which is of the same order of magnitude as the river inflow. No data are available to determine if this sediment builds up the shoals or is deposited on the accreting banks of the meanders.

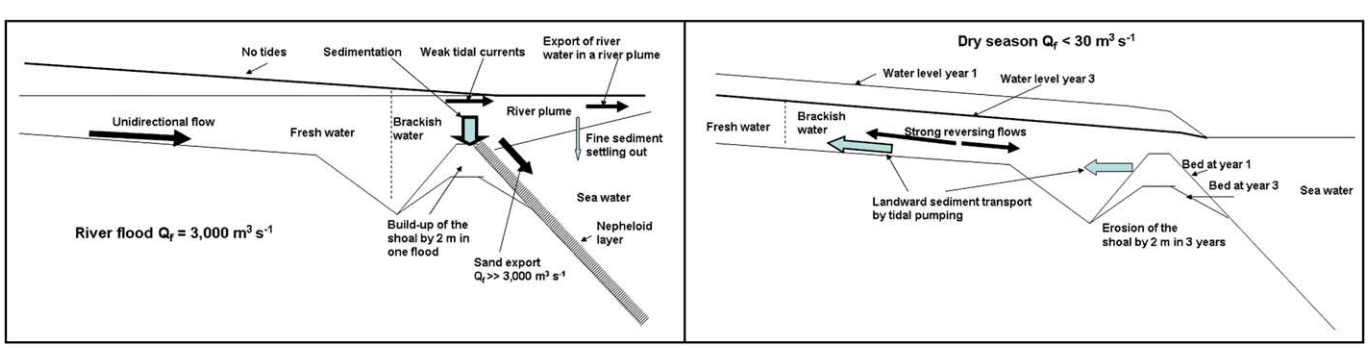

Fig. 11. Sketch of the dominant processes controlling the sediment pathways (shown as arrows) in the Daly Estuary (left) during a river flood in the wet season and (right) during the dry season.

The time scale for erosion of the shoal in the dry season can be estimated from the field data. At spring tides, the bed load velocity is 0.05 m s^{-1} landward and lasts 2 h. Assuming a lower estuary width of 500 m and a depth of bed load depth of 0.1–0.5 m, the landward bed load transport is 0.19–9 $\times 10^4$ ton $tide^{-1}$. The net, landward fine sediment load, calculated from the SSC, depth, and velocity data, is 2×10^5 ton $tide^{-1}$. Assuming 200 such tides per year, the landward sediment transport is 5.8×10^7 ton y^{-1}. To remove the 2 m thick cap from the shoals and redistribute it landward in the whole estuary take 3.4 years, a value in agreement with observations. When that sediment has been redistributed, the mean estuary bed on the average has been raised 0.1 m. Exceptionally large river floods (e.g. the 1956, 1974 and 1998 events) do not scour all the sediment out of the estuary. Instead they deposit much of it at the shoal offshore from the mouth. This sediment is then redistributed landward throughout the estuary by tidal pumping in the dry season. If all the riverine sediment remained trapped, the estuarine evolution time scale would be about 50 years, in agreement with the prediction of Wolanski (2006). The fate of sediment in large river floods remains unknown and deserves detailed investigations in view of the economic development pressure within the Daly River catchment.

Acknowledgments

It is a pleasure to acknowledge our colleagues at AIMS and NRETA, particularly Simon Spagnol, Cary Mclean and Errol Kerle; without their enthusiastic support the field study in this difficult environment would not have been possible. The study was facilitated by AIMS and NRETA.

References

Ayukai, T., Wolanski, E., 1997. Importance of biologically mediated removal of fine sediments from the Fly River plume, Papua New Guinea. Estuarine, Coastal and Shelf Science 44, 629–639.

Barry, K.M., Thieke, R.J., Mehta, A.J., 2006. Quasi-hydrodynamic lubrication effect of clay particles on sand grain erosion. Estuarine, Coastal and Shelf Science 67, 161–169.

Bryce, S., Larcombe, P., Ridd, P.V., 1998. The relative importance of landward-directed tidal sediment transport versus freshwater flood events in the Normanby River estuary, Cape York Peninsula. Marine Geology 149, 55–78.

Camenen, C., Larson, M., 2005. A general formula for non-cohesive bed load sediment transport. Estuarine, Coastal and Shelf Science 63, 249–260.

Chappell, J., 1993. Contrasting Holocene sedimentary geologies of the lower Daly River, northern Australia, and lower Sepik-Ramu, Papua New Guinea. Sedimentary Geology 83, 339–358.

Chappell, J., Ward, P., 1985. Seasonal tidal and freshwater chemistry of the South Alligator and Daly Rivers. In: Bardsley, K.N., Davie, J.D.S., Woodroffe, C.D. (Eds.), Coasts and Tidal Wetlands of the Australian Monsoon Region. Mangrove Monograph No. 1. Australian National University Northern Australia Research Unit, Darwin, pp. 97–108.

Chappell, J., Woodroffe, C.D., 1994. Macrotidal estuaries. In: Carter, R.W.G., Woodroffe, C.D. (Eds.), Coastal Evolution. Cambridge University Press, pp. 187–218.

Dyer, K.R., 1986. Coastal and Estuarine Sediment Dynamics. Wiley, Chichester, 342 pp.

Dyer, K.R., 2000. Estuaries, A Physical Introduction, second ed. John Wiley & Sons, 195 pp.

Fabricius, K., Wolanski, E., 2000. Rapid smothering of coral reef organisms by muddy marine snow. Estuarine, Coastal and Shelf Science 50, 115–120.

FitzGerald, D.M., Knight, J., 2005. High Resolution Morphodynamics and Sedimentary Evolution of Estuaries. Springer, Dordrecht, 364 pp.

FitzGerald, D.M., Buynevich, I.V., Fenster, M.S., Kelley, J.T., Belknap, D.F., 2005. Coarse-grain sediment transport in northern New England estuaries: a synthesis. In: FitzGerald, D.M., Knight, J. (Eds.), High Resolution Morphodynamics and Sedimentary Evolution of Estuaries. Springer, Dordrecht, pp. 195–213.

Kjerfve, B., 1994. Coastal Lagoon Processes. Elsevier, Amsterdam, 598 pp.

Milliman, J.D., Meade, R.H., 1983. World-wide delivery of river sediment to the oceans. Journal of Geology 91, 1–21.

Nittrouer, C.A., DeMaster, D.J., 1986. Sedimentary processes on the Amazon continental shelf: past, present and future research. Continental Shelf Research 6, 5–30.

Perillo, G.M.E., 2000. Geomorphology and Sedimentology of Estuaries. Elsevier, Amsterdam, 471 pp.

Postma, H., 1967. Sediment transport and sedimentation in the estuarine environment. In: Lauff, G.H. (Ed.), Estuaries. American Association for the Advancement of Science Publication 16. American Association for the Advancement of Science, Washington, DC, pp. 651–658.

Pritchard, D.W., 1952. Salinity distribution and circulation in the Chesapeake estuarine system. Journal of Marine Research 11, 106–123.

Pritchard, D.W., 1967. What is an estuary? Physical viewpoint. In: Lauff, G.H. (Ed.), Estuaries. American Association for the Advancement of Science Publication 83. American Association for the Advancement of Science, Washington, DC, pp. 3–5.

Syvitski, J.P.M., Harvey, N., Wolanski, E., Burnett, W.C., Perillo, G.M.E., Gornitz, V., 2005. Dynamics of the coastal zone. In: Crossland, C.J., Kremer, H.H., Lindeboom, H.J., Marshall Crossland, J.I., Le Tissier, M.D.A. (Eds.), Coastal Fluxes in the Anthropocene. Springer-Verlag, Berlin, pp. 39–94.

Tricker, R.A.R., 1965. Bores, Breakers, Waves and Wakes: An Introduction to the Study of Waves on Water. Miles and Boon Limited, London.

Vertessy, R.A., 1990. Morphodynamics of macrotidal rivers in far northern Australia. PhD thesis, Department of Biogeography and Geomorphology, Australian National University, Australia, 351 pp.

White, L., Legat, V., Deleersnijder, E., Le Roux, D.Y., 2006. A one-dimensional benchmark for the propagation of Poincaré waves. Ocean Modelling, in press.

Wolanski, E., 2006. The evolution time scale of macro-tidal estuaries: examples from the Pacific Rim. Estuarine, Coastal and Shelf Science 66, 544–549.

Wolanski, E., Spagnol, S., 2003. Dynamics of the turbidity maximum in King Sound, tropical Western Australia. Estuarine, Coastal and Shelf Science 56, 877–890.

Wolanski, E., Williams, D., Spagnol, S., Chanson, H., 2004. Undular tidal bore dynamics, Daly Estuary, Australia. Estuarine, Coastal and Shelf Science 60, 629–636.

Woodroffe, C.D., 2003. Coasts, Form, Process and Evolution. Cambridge University Press, 623 pp.